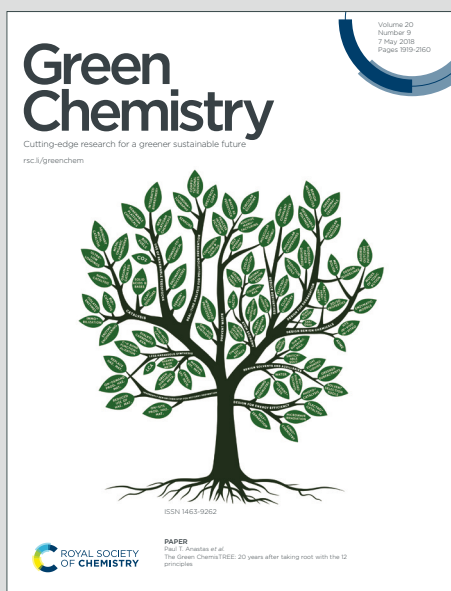


Green Chemistry

Cutting-edge research for a greener sustainable future

Accepted Manuscript

This article can be cited before page numbers have been issued, to do this please use: F. Niu, M. Bahri, O. Ersen, B. Kusema, Z. Yan, A. Khodakov and V. Ordonsky, *Green Chem.*, 2020, DOI: 10.1039/D0GC00937G.



This is an Accepted Manuscript, which has been through the Royal Society of Chemistry peer review process and has been accepted for publication.

Accepted Manuscripts are published online shortly after acceptance, before technical editing, formatting and proof reading. Using this free service, authors can make their results available to the community, in citable form, before we publish the edited article. We will replace this Accepted Manuscript with the edited and formatted Advance Article as soon as it is available.

You can find more information about Accepted Manuscripts in the [Information for Authors](#).

Please note that technical editing may introduce minor changes to the text and/or graphics, which may alter content. The journal's standard [Terms & Conditions](#) and the [Ethical guidelines](#) still apply. In no event shall the Royal Society of Chemistry be held responsible for any errors or omissions in this Accepted Manuscript or any consequences arising from the use of any information it contains.

Multifaceted Role of Mobile Bismuth Promoter in Alcohol Amination over Cobalt Catalysts

Feng Niu^{a,b}, Mounib Bahri^c, Ovidiu Ersen^c, Zhen Yan^b, Bright T. Kusema^b, Andrei Y. Khodakov^{a*} and Vitaly V. Ordonsky^{a,b*}

^a Univ. Lille, CNRS, Centrale Lille, ENSCL, Univ. Artois, UMR 8181 - UCCS - Unité de Catalyse et Chimie du Solide, F-59000 Lille, France

^b E2P2L, UMI 3464 CNRS-Solvay, 3966 Jin Du Rd., 201108 Shanghai, China

^c Institut de Physique et Chimie des Matériaux de Strasbourg (IPCMS)-UMR 7504 CNRS, Université de Strasbourg, 23 rue du Loess, BP 43-67034 Strasbourg Cedex 2, France

*Corresponding authors: Andrei Khodakov E-mail: andrei.khodakov@univ-lille.fr;
Vitaly Ordonsky E-mail: vitaly.ordonsky-ext@solvay.com

Abstract

View Article Online
DOI: 10.1039/D0GC00937G

Promotion with small amounts of different elements is an efficient strategy for the enhancement of the performance of many heterogeneous catalysts. Supported cobalt catalysts exhibit significant activity in the synthesis of primary amines via alcohol amination with ammonia, which is an economically efficient and environmentally friendly process. Insufficient selectivity to primary amines, low activity and fast cobalt catalyst deactivation remain serious issues restricting application of alcohol amination in the industry.

In this work, we have discovered the multifaceted role of the bismuth promoter, which is highly mobile under the reaction conditions, in 1-octanol amination over supported cobalt catalysts. First, the overall reaction rate was enhanced more than twice on the promotion with bismuth. Second, the selectivity to primary amine increased 6 times in the presence of Bi at high alcohol conversion. Finally, the bismuth promotion resulted in the extremely high stability of the cobalt catalyst. Characterization by XRD, temperature programmed reduction, STEM, CO chemisorption, BET, TGA and FTIR has showed that the enhancement of the catalytic performance on the promotion with bismuth is due to better cobalt reducibility, easy removal of strongly adsorbed intermediates and products by the mobile promoter and steric hindrances for amine coupling reactions resulting in secondary and tertiary amines.

Introduction

Amines are important materials in chemical industry and life science [1]. Most aliphatic amines and their derivatives are essential intermediates for organic synthesis, which are widely used in the production of agrochemicals, pharmaceuticals, organic dyes, detergents, fabric softeners, surfactants, corrosion inhibitors, lubricants, polymers and so on [2,3].

A number of routes for amines synthesis have been developed like Hofmann alkylation, Buchwald-Hartwig and Ullmann reactions, hydroamination, reduction of nitriles, and reductive amination [4,5,6,7,8,9,10,11]. Most of currently available amine synthesis routes involve generation of by-side products harmful for environment and human health. Direct one-pot amination of alcohols with ammonia is a safe method of amine synthesis with the environmentally benign byproduct such as water. This route of amination corresponds to the most part of the principles of Green Chemistry like prevention, atom economy, safer chemicals, no solvents, catalysis, reduce derivatives etc.

The alcohol amination on different supported metallic catalysts, such as Ru [12], Ni [13] and Co [14], under hydrogen can be achieved via so called hydrogen borrowing or hydrogen auto transfer methodology [15,16,17,18], which consists of dehydrogenation and hydrogenation processes. The one-pot alcohol amination generally consists of three consecutive steps: (i) dehydrogenation of an alcohol to a reactive aldehyde (or ketone); (ii) imine formation by coupling of a carbonyl compound with ammonia; (iii) amine formation by hydrogenation of the imine over the catalyst.

During the whole process, water is the only by-product, which emphasizes the advantage of this environmental friendly route. The alcohol amination catalysts however, usually suffer from the low selectivity to primary amines [19]. Insufficient activity and fast catalyst deactivation significantly restrict application of the alcohol amination in the industry [20]. Hydrogen pressure during the amination reaction is essential to prevent catalyst deactivation. Amines in the hydrogen borrowing mechanism are produced by hydrogenation of imines. An increase in the selectivity to primary amine during alcohol amination in the presence of hydrogen can be due to the faster imine hydrogenation [21].

Our previous report indicates structure-insensitive character of amination reaction over ruthenium nanoparticles, but strong structure sensitivity of the primary amine coupling to secondary amine. The rate of primary amine coupling rapidly increases with the increase in the ruthenium particle size. A combination of structure insensitive alcohol amination and structure sensitive primary amine coupling results in a significant increase in the selectivity to primary amines with decrease in the size of metal nanoparticles [12].

Different approaches have been used to control the activity and selectivity in amination of alcohols. In our previous work [14], intentional deposition of polymeric carbonaceous species on the surface of Co/Al₂O₃ catalysts was used to considerably improve the selectivity of primary amines in the gas and liquid-phase amination of aliphatic alcohols with NH₃. The selectivity enhancement was attributed to the suppression of primary amine self-coupling because of hindering of secondary imine

hydrogenation. Addition of secondary metals to the parent cobalt catalyst was shown to be an efficient way to enhance the reaction activity and selectivity. Fischer et al. [22] reported the catalytic synthesis of 1, 3-diaminopropane from 1, 3-propanediol and ammonia in a continuous fixed-bed reactor using unsupported Co-based catalysts. Promotion of the unsupported cobalt catalyst with iron or lanthanum significantly improved the selectivity of 1,3-diaminopropane. The effect has been assigned to suppression of the transformation of active metastable β -cobalt phase to the thermodynamically more stable α -cobalt phase under reaction conditions, which improved the catalytic selectivity. Takanashi et al. investigated the synergetic effect between rhodium and indium for the amination of 1,2-propanediol [23]. The obvious catalytic rate promotion was mainly attributed to the electronic perturbation of Rh sites by indium that weakens the binding of ammonia. Wang et al. [24] combined DFT calculations, scaling relations, kinetic simulations and catalysis experiments to determine the key factors that govern the activity and selectivity of metal catalysts for the direct amination of alcohols with ammonia. They uncovered that addition of Ag or Ru into supported Co catalyst led to the most promising catalysts.

Traditionally metallic or non-metallic promoters are considered immobile on the catalyst surface and play a static role with local modification of the active sites [25,26,27]. Recently, we have discovered strong promoting effects of low melting point metal promoters such as Bi and Pb [28,29] in Fischer-Tropsch synthesis over Fe and Co catalysts. An exceptional increase in the reaction rate (up to 10 times), higher selectivity to light olefins (up to 60 %) and enhanced stability have been observed over

Fe catalysts in high temperature Fischer-Tropsch synthesis. These effects have been assigned to a pseudo-liquid state of the promoters under the reaction conditions, their intensive migration, redox cycles during the reaction and close contact between metal and the promoters. We have also found that the presence of Bi promoter significantly improves stability of the cobalt and nickel catalysts in low temperature Fischer-Tropsch synthesis [29].

In this paper, we uncovered multiple effects of the bismuth promoter on the cobalt catalysts in the amination of alcohols. A significant increase in the activity, higher selectivity to primary amines and enhanced stability were observed (**Figure 1**).

Results and Discussion

Enhancement of catalytic performance on bismuth promotion

The Co/Al₂O₃ catalysts with the Bi promoter content in the range from 0 to 5 wt% were prepared by impregnation with subsequent calcination and reduction at 450 °C. They were used for the synthesis of primary 1-octylamine directly from 1-octanol and ammonia in the presence of hydrogen in a batch reactor. Note that no 1-octanol conversion was observed in a blank experiment without catalyst addition.

Direct liquid phase amination of alcohol with ammonia over supported cobalt catalyst follows the hydrogen borrowing mechanism (**Figure 2**). Generally, the rate determining step is catalytic dehydrogenation of alcohol to corresponding aldehyde [30, 31, 32]. Condensation of octanal with ammonia is a fast non-catalytic reaction leading to formation of hemiaminal followed by elimination of water to produce primary imines [33]. Finally, hydrogenation of imines leads to the formation of primary amines. The

selectivity to primary amines sharply decreases at high conversion, because of self-coupling of primary amine to secondary and tertiary amines.

The catalytic performance data for liquid phase amination of 1-octanol over the catalysts before and after Bi addition to Co are displayed in **Figure 3a** and **Figure S1, SI**. For the Co_{0.5}Bi/Al₂O₃ catalyst, the catalytic conversion and reaction rate were ~2.3 times higher than those of fresh catalyst without Bi promotion (81 % and 0.105 mol_{octanol}·g_{Co}⁻¹·h⁻¹ versus 38 % and 0.046 mol_{octanol}·g_{Co}⁻¹·h⁻¹ respectively). This indicates that Bi addition to the cobalt catalysts largely increases the amination activity. As the Bi loading content increased from 0.5 to 5 wt%, the 1-octanol conversion gradually decreased from 81 % to 14.4 %. Higher Bi loading leads to lower reaction rate probably because of the decrease in the amount of accessible Co atoms for the catalytic reaction. For comparison, a pure Bi/Al₂O₃ catalyst was also tested and showed a low conversion of 4.5 %. This reveals that Co metal is the main active phase for 1-octanol amination in the non-promoted and bismuth promoted cobalt catalysts.

It is interesting to note that a mechanical mixture of Co/Al₂O₃ and Bi/Al₂O₃ exhibited 61% conversion, which is much higher in comparison with Co/Al₂O₃. In the mechanical mixture, because of spatial separation, no interaction between cobalt and bismuth species could be expected. Bismuth has a low melting temperature (271 °C). It can be therefore, in the liquid state during catalyst activation, which was conducted at 450 °C. Alcohol amination was performed over the cobalt catalyst at the temperature higher than the Tammann temperature of metallic bismuth. This suggests that some bismuth mobility can take place even during the reaction at 180 °C. Higher reaction

rate observed over the mechanical mixture of alumina supported cobalt and bismuth catalysts proves high mobility of metallic Bi on the surface of Co under reaction conditions.

The selectivity-conversion curves for amination of 1-octanol over Co catalysts before and after the Bi promotion with different loading content are shown in **Figure 3b**. Different 1-octanol conversions were obtained by varying the reaction time from 0 h to 48 h. The freshly activated sample Co/Al₂O₃ displays 90 % selectivity to 1-octylamine at the conversion of 20 %. As the conversion increases to nearly 100 %, the selectivity to 1-octylamine dramatically decreases to 11 %, which is similar to the reported results in both gas phase and liquid phase amination of alcohols due to the self-coupling of primary amines to secondary and tertiary amines (**Figure 2**) [16]. Surprisingly, the bismuth promotion of cobalt catalysts produces a strong effect on the selectivity especially at high 1-octanol conversion. The selectivity to 1-octylamine gradually increases (at the same 1-octanol conversion) as Bi loading content increases. The optimal selectivity at higher conversion over Co_{5.0}Bi/Al₂O₃ catalyst increases to 66 %, which is 6 times higher than that of freshly activated Co/Al₂O₃. Thus, the selectivity to primary 1-octylamine during liquid phase amination of 1-octanol can be controlled by adjusting the Bi content.

The catalytic stability data for liquid phase amination of 1-octanol over freshly activated Co/Al₂O₃ and Bi-promoted Co_{1.0}Bi/Al₂O₃ are shown in **Figure 4**. After 3 catalytic amination cycles, for the freshly activated Co/Al₂O₃ catalyst, 1-octanol conversion sharply drops from 36 % to 8 %. Interestingly, for the Bi-promoted Co

catalyst, conversion decreased only very slightly, which indicates higher stability and reusability. ICP analysis suggests that no leaching of Bi has been observed after 3 cycles (**Table S1, SI**). Thus, the Bi promoter has positive effects on overall activity, selectivity to primary amines and stability of the Co based catalysts in the 1-octanol amination.

Catalyst characterization

N₂ adsorption-desorption and BET results show similar surface area and pore size for the calcined Co/Al₂O₃ and Co_xBi/Al₂O₃ catalysts (**Table 1**). **Figure 5a** displays the XRD patterns of all samples. The calcined Co/Al₂O₃ and Bi/Al₂O₃ catalysts exhibit the presence of Co₃O₄ and Bi₂O₃ phases, respectively. For the Bi promoted Co catalysts, XRD peaks corresponding to the Bi₂O₃ phase gradually appear as the loading content of Bi increased from 0.5 wt% to 5.0 wt% and reached highest intensity for Co_{5.0}Bi/Al₂O₃. The average particle size of Co₃O₄ calculated by Scherrer equation using X-ray line broadening method was around 10 nm for the fresh non-promoted and Bi promoted Co catalysts as well as for the one after amination reaction (**Table 1**). The particle sizes measured by XRD were consistent with STEM results calculated from particle size distribution (**Figure 6, Figure S2**). Therefore, no obvious modification of Co particle size and distribution occur after the Bi promotion.

Ex-situ XPS analyses of Co_{1.0}Bi/Al₂O₃ before and after reduction and amination have provided further information about the bismuth and cobalt phases (**Figure S3, SI**). The Co 2p binding energies, spin-orbital splitting and low intense shake-up satellite structure indicate [34, 35] the presence of Co₃O₄ phase in Co/Al₂O₃ and Co_{1.0}Bi/Al₂O₃.

Bi 4f XPS suggests the presence of Bi in the form of Bi_2O_3 in the catalysts (**Figure S3b, SI**). It is interesting to note that after the amination reaction, the peak shifts to lower binding energy, which can be explained by strong interaction of Bi with Co with partial reduction of Bi oxide.

The localization of Bi promoter for the $\text{Co}_{1.0}\text{Bi}/\text{Al}_2\text{O}_3$ catalyst after pretreatment was further investigated using HAADF-STEM and corresponding EDX mapping. As shown in **Figure 6**, the Bi promoted Co catalyst exhibits a broad size distribution of agglomerated Co nanoparticles in the range of 5 to 20 nm (**Figure S2, SI**). The EDX mapping graph in **Figure 6a** clearly shows that Bi is localized in the close proximity to Co nanoparticles. The localization of Bi and Co can be observed by HR STEM analysis (**Figure S4, SI**). The prepared catalyst contains Bi oxide particles distributed over Co_3O_4 nanoparticles. Reduction of the catalyst leads to sintering of Bi to large particles, however, after the amination reaction Bi forms a 2-3 nm layer over Co surface (**Figure S4, SI**).

The high mobility of Bi has been also confirmed by EDX analysis of mechanical mixture before and after catalysis. Localization of Bi and Co is different for the mechanical mixture before reaction (**Figure 6**). Catalyst activation and catalytic reaction induce migration of liquid Bi to the surface of Co nanoparticles according to EDX mapping (**Figure 6**).

The reducibility of Co before and after Bi promotion was investigated by H_2 -TPR technique. As shown in **Figure 5b**, the TPR profile of oxidized $\text{Co}/\text{Al}_2\text{O}_3$ depicts two

hydrogen consumption peaks at 335 and 622 °C. The first peak at 335 °C corresponds to the reduction process of $\text{Co}_3\text{O}_4 \rightarrow \text{CoO} \rightarrow \text{Co}$, while the broad reduction peak at 622 °C mostly due to the reduction of Co-Al mixed oxide phases [36, 37]. After Bi promotion, the $\text{Co}_x\text{Bi}/\text{Al}_2\text{O}_3$ catalysts exhibit extra hydrogen consumption peaks at 270-310 °C, which corresponds to the reduction of Bi_2O_3 and Co_3O_4 in proximity to Bi_2O_3 . At the same time, the Co_3O_4 reduction peak shifts to higher temperatures in comparison with non-promoted catalyst (from 335 to ~350 °C) with increase in the Bi content. The peak shift can be explained by more difficult cobalt reducibility in the presence of bismuth. Interestingly, the broad reduction peak at 622 °C corresponding to the formation of barely reducible cobalt-alumina mixed oxides observed in $\text{Co}/\text{Al}_2\text{O}_3$ disappears for all $\text{CoBi}/\text{Al}_2\text{O}_3$ catalysts. This could indicate weakening interactions between cobalt species and alumina support and a smaller fraction of barely reducible cobalt aluminate in the Bi-promoted catalysts.

Cobalt metal dispersion and surface area were evaluated using CO adsorption in a pulse mode after *in-situ* reduction for all samples. Note that there was no CO adsorption on activated $\text{Bi}/\text{Al}_2\text{O}_3$. The freshly reduced $\text{Co}/\text{Al}_2\text{O}_3$ catalyst shows relatively low carbon monoxide adsorption (1.14 mmol CO/mmol Co). The CO adsorption over the bismuth promoted catalysts gradually decreased from 1.14 to 0.18 mmol CO/mmol Co caused by increasing Bi content. The variation of CO adsorption as a function of Bi content was consistent with the observed decrease in the catalytic activity (**Figure 2**).

Mechanism of bismuth promotion

Catalyst characterization was indicative of the appearance of new low temperature

peaks in the TPR profiles (**Figure 5**) related to easily reducible cobalt species and decrease in the fraction of barely reducible mixed cobalt alumina species after the promotion with bismuth. Thus, the increase in the amination rate could be at least partially attributed to the reducibility enhancement.

Numerous previous kinetic studies [30, 31, 32] suggest that dehydrogenation of alcohol is the rate limiting step for amination reaction over metal catalysts [38] (**Figure 2**). To investigate the effect of Bi over this step, liquid phase dehydrogenation of 2-octanol to 2-octanone was tested over activated Co/Al₂O₃ and bimetallic Co_xBi/Al₂O₃ catalysts. As shown in **Figure 7**, the conversion was only 2.8 % for freshly activated Co catalyst [39]. The conversion of alcohol increased to 16 % after addition of promoter, which corresponds to thermodynamic equilibrium. The conversion gradually decreases from 16 % to 1 % when Bi loading content increases from 0.5 to 5 wt%, which is consistent with the activity enhancement effect for 1-octanol amination. Thus, this experiment confirms that the limiting step of amination over metal catalysts such as alcohol dehydrogenation (**Figure 2**) is enhanced over the Bi-promoted Co catalysts. Higher Bi content suppresses the activity in both dehydrogenation and amination reaction.

It is known that carbonyl compound produced on the alcohol dehydrogenation can poison cobalt active surface and result in the significant decrease in the catalytic activity [40]. Thus, possible explanation of the enhancement of alcohol dehydrogenation step in the presence of Bi could be continuous regeneration of the surface of Co by the removal of adsorbed amines, alcohol and aldehydes. In order to prove this assumption,

amination of 1-octanol was performed after preliminary poisoning of Co/Al₂O₃ by CO adsorption. The activity of freshly activated non-promoted cobalt catalysts sharply decreased after CO poisoning, while there was no effect of carbon monoxide pre-adsorption on the Bi-promoted Co catalyst (**Figure S5, SI**). Increase in the activity could be explained by easy carbon monoxide removal by the mobile Bi promoter. The observed phenomenon is similar to our earlier findings [29]. Indeed, the temperature of 1-octanol amination is higher than the bismuth Tammann temperature.

It is widely accepted that secondary and tertiary amines can form accordingly to two mechanisms: amination of remaining 1-octanol with 1-octylamine or self-coupling reaction of 1-octylamine through condensation of primary amines with corresponding imines. Amination of 1-octanol with 1-octylamine can be observed at low or medium conversions, while 1-octylamine self-coupling reaction seems to be the main reason for selectivity loss at high 1-octanol conversion (**Figure 2**). To investigate the effect of Bi addition on the selectivity enhancement during liquid phase amination, 1-octylamine coupling to dioctylamine and trioctylamine was conducted at relatively low 1-octylamine conversion (< 10%). **Figure 8** shows the distribution of 1-octylamine converted products over freshly activated Co/Al₂O₃ and Bi-promoted catalysts. The main products of 1-octylamine coupling were secondary imines and amines. The selectivity to secondary imine increases and the selectivity to secondary amine decreases with increase in the Bi content in the catalyst.

The calculated TOF for 1-octylamine self-coupling reaction gradually decreased from 365 to 148 h⁻¹ after Bi promotion (**Table S2, SI**). The TOF numbers for 1-octanol

amination for all the catalysts were about 210 h^{-1} . Thus, the ratio of TOF (1-octylamine coupling)/TOF (1-octanol amination) is about 2.5 times higher for non-promoted Co catalyst in comparison with $\text{Co}_5.0\text{Bi}/\text{Al}_2\text{O}_3$. This result demonstrates that the reaction rate of 1-octylamine self-coupling over Bi promoted surface Co sites was much lower than that of 1-octanol amination to 1-octylamine resulting. Consequently, the selectivity to primary amine has increased. Steric hindrance during hydrogenation of secondary imine induced by Bi on the surface of Co results in suppression of hydrogenation of bulky secondary imine with shift of the reaction selectivity to primary amine. The similar effect has been observed during amination of alcohols over Co nanoparticles after their pretreatment with alcohol resulting in carbon deposition. [14].

Usually, Co based catalysts can be easily deactivated by surface residuals as well as being oxidized to Co oxides during catalytic reactions [41, 42, 43]. The presence of Bi had significant effect on the enhancement of the stability of Co catalyst during amination reaction (**Figure 3**). TGA (**Figure S6, SI**) and FTIR (**Figure S7, SI**) techniques were used to investigate both fresh and Bi promoted Co catalysts before and after the amination test. TG analysis exhibits a total weight loss of about 8 wt% for $\text{Co}/\text{Al}_2\text{O}_3$ catalyst after reaction and nearly half of that for Bi promoted Co catalyst (~4 wt%). Analysis of FTIR spectra indicates the presence of carbonaceous species with C-H stretching vibrations at 2965 and 2910 cm^{-1} in $-\text{CH}_3$ and $-\text{CH}_2$ groups, respectively in the spectra of both non-promoted and Bi-promoted catalysts. The C-N stretching vibration of aliphatic amines is observed by the band at 1250 cm^{-1} . Thus, deposition of amines and their derivatives over Co metal surface could deactivate the supported Co

catalyst. Regeneration of the catalyst by calcination and reduction results in increase of the catalytic activity of Co/Al₂O₃ to the initial level indicating on the key role of poisoning in deactivation of the catalyst (**Figure 4**). Note that no noticeable deactivation was observed for the Bi-promoted catalysts after 3 consecutive reaction cycles. The presence of Bi on the surface of the catalyst seems to reduce deposition of carbon species due to higher mobility and continuous removal of these species by Bi.

Conclusion

The promotion of alumina supported cobalt catalysts with bismuth results in multiple effects on the catalyst structure and performance in alcohol amination. First, the promotion with bismuth results in weakening cobalt-alumina interaction and lower fraction of barely reducible cobalt aluminates. The increase in the amination activity in the presence of Bi is also due the promotion of dehydrogenation reaction by desorption of adsorbed poisoning species. Second, the increase in the selectivity to primary amine after the Bi addition is a result of suppression of 1-octylamine self-coupling reaction by hindering of bulky secondary imine hydrogenation. Furthermore, the high stability of Bi promoted Co catalyst has been attributed to the easy removal of strongly adsorbed carbon species from the catalyst surface by mobile bismuth species. The promotion of alumina supported cobalt catalyst with bismuth results in a novel versatile bimetallic Co_xBi/Al₂O₃ catalyst with high activity, selectivity and stability for liquid phase amination of alcohols with ammonia.

Methods

Reagents

All the commercial reagents were used without any purification. Commercial γ - Al_2O_3 (SASOL, PURALOX SCCa-5/170, D50: 50 μm -100 μm) was used as a catalytic support. Cobalt(II) nitrate hexahydrate ($\text{Co}(\text{NO}_3)_2 \cdot 6\text{H}_2\text{O}$, >99%) and bismuth(III) nitrate pentahydrate ($\text{Bi}(\text{NO}_3)_3 \cdot 5\text{H}_2\text{O}$, >98%) supplied by Sigma-Aldrich, were used as impregnation precursors for synthesis of metallic and bimetallic active phases loaded on the support. 1-Octanol ($\text{C}_8\text{H}_{18}\text{O}$, >99.5%), 1-octylamine ($\text{C}_8\text{H}_{19}\text{N}$, >99.5%), di-1-octylamine ($\text{C}_{16}\text{H}_{35}\text{N}$, >99.5%), tri-1-octylamine ($\text{C}_{24}\text{H}_{51}\text{N}$, >99.5%), 2-octanol ($\text{C}_8\text{H}_{18}\text{O}$, >99.5%), 2-octanone ($\text{C}_8\text{H}_{16}\text{O}$, 98%), toluene (C_7H_8 , >99.5%), biphenyl ($\text{C}_{12}\text{H}_{10}$), 1-pentanol ($\text{C}_5\text{H}_{12}\text{O}$, >99.5%), benzyl alcohol ($\text{C}_7\text{H}_8\text{O}$, >99%), furfuryl alcohol ($\text{C}_5\text{H}_6\text{O}_2$, >99%), supplied by Sigma-Aldrich, were used as reactants and standards for GC calibration. Hydrogen and ammonia supplied by Air Liquide were used in the catalytic amination test.

Preparation of supported Co and bimetallic CoBi catalysts

$\text{Co}/\text{Al}_2\text{O}_3$, $\text{Bi}/\text{Al}_2\text{O}_3$ and $\text{Co}_x\text{Bi}/\text{Al}_2\text{O}_3$ catalysts were prepared through incipient wetness impregnation and co-impregnation (IWI) of γ - Al_2O_3 using an aqueous solutions of cobalt nitrate hexahydrate [$\text{Co}(\text{NO}_3)_2 \cdot 6\text{H}_2\text{O}$] and bismuth(III) nitrate pentahydrate [$\text{Bi}(\text{NO}_3)_3 \cdot 5\text{H}_2\text{O}$], where x represents the weight percentage of Bi ($x = 0.5, 1.0, 2.0, \text{ and } 5.0$). The weight percentage of Co for all the samples was kept 10 wt%. The impregnated samples were dried in an oven at 80 °C for overnight and calcined in air with a heating ramp of 2 °C $\cdot\text{min}^{-1}$ from 25 °C to 500 °C to get the oxidized catalysts. All the catalysts were activated under a pure H_2 flow at 450 °C for 2 h before

each amination test. The Co/Al₂O₃ and Co_{1.0}Bi/Al₂O₃ catalysts after amination test were labeled as Co/Al₂O₃-AA and Co_{1.0}Bi/Al₂O₃-AA, respectively. To evaluate the level of deactivation resistance for fresh and Bi promoted Co catalysts, the Co/Al₂O₃ and Co_{1.0}Bi/Al₂O₃ catalysts were poisoned by CO chemisorption using CO pulses on the Micromeritics AutoChem instrument before amination test.

Characterization

The *ex situ* XRD patterns were measured by an X-ray diffractometer (D5000, Siemens) using Cu K α radiation ($\lambda = 0.15418$ nm). The scans were recorded in 2θ range from 10° to 80° using a step size of 0.02° and a step time of 5 s. The catalysts for measurement were all in oxide state without reduction in hydrogen. The average Co₃O₄ was calculated by Scherrer equation using X-ray line broadening method, which could be used for calculation of metallic cobalt size by the formula: $d(\text{Co}^0) = 0.75 d(\text{Co}_3\text{O}_4)$.

Hydrogen temperature-programmed reduction (H₂-TPR) was performed using a Micromeritics AutoChem II 2920 V3 0.2 apparatus equipped with a thermal conductivity detector (TCD) using ~60 mg sample. The thermal profiles were measured from room temperature to 800 °C with a temperature ramp of 5 °C·min⁻¹ under a 5 v/v% H₂/Ar flow [10 mL(STP)/min].

Scanning transmission electron microscopy (STEM) characterization in the high-angle annular dark-field (HAADF) mode was performed using a Cs-corrected JEOL JEM-2100F microscope operated at 200 keV with an EDX mapping detector from JEOL Silicon Drift Detector (DrySD60GV: sensor size 60 mm²).

The Agilent 720-ES ICP-OES combined with a Vulcan 42S robot was used for

determining the metal loading in the catalyst before and after amination reaction. View Article Online
DOI: 10.1039/D0GC00937G

BET specific surface areas and pore size were measured from the N₂ adsorption-desorption isotherms at 77 K on an automated gas sorption analyzer Micromeritics ASAP 2010.

Thermogravimetric analysis (TGA) of fresh and used catalysts was carried out using Mettler Toledo SMP/PF7458/MET/600W instrument under air flow [10 mL(STP)/min] in the temperature range of 20-900 °C using a heating rate of 5 °C·min⁻¹.

Ex situ Fourier transform-infrared (FT-IR) measurement of fresh and used catalysts was carried out on a Perkin-Elmer 1720 spectrometer using an Attenuated Total Reflectance (ATR) detector.

Ex situ X-ray photoelectron spectrometry (XPS) was carried out using a PHI 5000 Versa Probe X-ray photoelectron spectrometer with Al K α radiation. C 1s (284.6 eV) was used to calibrate the peak position.

Catalytic amination tests

The catalytic performance of the prepared freshly activated and Bi promoted Co catalysts was evaluated in the liquid-phase amination of 1-octanol with NH₃, which was carried out in a 30-mL stainless steel autoclave geared with a pressure gauge and a safety rupture disk. In a typical experiment, the autoclave reactor was charged with 0.84 g of 1-octanol and catalyst (~100 mg). No solvent was used in the test. Then, the reactor was sealed and evacuated by applying vacuum followed by charging NH₃ (~7 bar) and H₂ (~3 bar) into the reactor as reported earlier to keep catalyst in reduced form and fast

catalyst deactivation by adsorbed amines [38]. Finally, the reactor was placed on a hot plate equipped with a magnetic stirrer (500 rpm) at 180 °C for 0-48 h. The nominal 1-octanol/NH₃/H₂ molar ratio in the reactor was kept at 1/4.5/0.85. After the amination reaction, the reactor was cooled down to room temperature, and the mixture was filtrated and analyzed on an Agilent 7890 GC equipped with a HP-5 capillary column using biphenyl as the internal standard for calculation of conversion and selectivity. For catalytic stability test, after each amination reaction, the used catalyst was washed with ethanol and water and separated by centrifugation for several times and dried at 80 °C under vacuum for 10 h for retest. After 3 cycles, the used catalysts were calcined at 400 °C under air to remove surface cokes followed by hydrogenation at 450 °C for further amination test.

Catalytic model reactions

The liquid-phase self-coupling of 1-octylamine and dehydrogenation of 2-octanol over the freshly activated and Bi promoted Co catalysts were conducted in the same autoclave reactor. Typically, for coupling reaction, the reactor was charged with 1 mL 1-octylamine, 20 mg of catalysts, and nominal 1-octylamine/NH₃/H₂ molar ratio was kept at 1/4.5/0.85. The reaction was performed at 180 °C for 0-4 h. No solvent was either used during the self-coupling reaction. For dehydrogenation reaction, conditions were as follows: 2-octanol 50 mg, toluene 1 g in the presence of catalyst 50 mg. The reaction was performed at 140 °C for 15 h.

Supporting Information

Catalytic reaction rate, TGA, FTIR, STEM, XPS, HRTEM, ICP-OES and TOF values. View Article Online
DOI: 10.1039/D0GC00937G

Data availability

All data are available from the authors upon reasonable request.

Acknowledgment

The authors thank Solvay for financial support of this work. Chevreul Institute (FR 2638), Ministère de l'Enseignement Supérieur, de la Recherche et de l'Innovation, Hauts-de-France Region and FEDER are acknowledged for supporting and funding partially this work.

References

- 1 J. Magano and J. R. Dunetz, *Chem. Rev.*, 2011, **111**, 2177-2250.
- 2 G. Heilen, H. J. Mercker, D. Frank, R. A. Reck and R. Jäck, in: W. Gerhertz (Ed.), *Ullmanns Encyclopedia of Industrial Chemistry*, vol. 2A, fifth ed., VCH, Weinheim, 1985, pp. 1-18.
- 3 H. A. Wittcoff, B. G. Reuben, and J. S. Plotkin, *Industrial Organic Chemicals*. (3rd edition, Wiley, Hoboken, N.J, 2013).
- 4 Q. Xu, H. M. Xie, E. L. Zhang, X. T. Ma, J. H. Chen, X. C. Yu and H. Li, *Green Chem.*, 2016, **18**, 3940-3944.
- 5 T. E. Müller, K. C. Hultsch, M. Yus, F. Foubelo and M. Tada, *Chem. Rev.*, 2008, **108**, 3795-3892.
- 6 T. Senthamarai, K. Murugesan, J. Schneidewind, N. V. Kalevaru, W. Baumann, H. Neumann, P. C. J. Kamer, M. Beller and R. V. Jagadeesh, *Nat. Commun.*, 2018, **9**, 4123.
- 7 R. Reguillo, M. Grellier, N. Vautravers, L. Vendier and S. Sabo-Etienne, *J. Am. Chem. Soc.*, 2010, **132**, 7854-7855.
- 8 M. T. Pirnot, Y. M. Wang and S. L. Buchwald, *Angew. Chem. Int. Ed.*, 2016, **55**, 48-57.
- 9 B. R. Brown, *The Organic Chemistry of Aliphatic Nitrogen Compounds*. (Oxford University Press, NY, 1994).
- 10 P. Zhou, Z. H. Zhang, L. Jiang, C. L. Yu, K. L. Lv, J. Sun and S. G. Wang, *Appl. Catal. B*, 2017, **210**, 522-532.
- 11 P. Zhou, L. Jiang, F. Wang, K. J. Deng, K. L. Lv and Z. H. Zhang, *Sci. Adv.*, 2017, **3**, e1601945.

- 12 G. F. Liang, Y. G. Zhou, J. P. Zhao, A. Y. Khodakov and V. V. Odomsky, *ACS Catal.*, 2018, **8**, 11226-11234.
- 13 A. Y. K. Leung, K. Hellgardt and K. K. Hii, *ACS Sustainable Chem. Eng.*, 2018, **6**, 5479-5484.
- 14 F. Niu, S. H. Xie, M. Bahri, O. Ersen, Z. Yan, B. T. Kusema, M. Pera-Titus, A. Y. Khodakov and V. V. Odomsky, *ACS Catal.*, 2019, **9**, 5986-5997.
- 15 A. Corma, J. Navas and M. J. Sabater, *Chem. Rev.*, 2018, **118**, 1410-1459.
- 16 O. Saidi, A. J. Blacker, M. M. Farah, S. P. Marsden and J. M. J. Williams, *Angew. Chem. Int. Ed.*, 2009, **48**, 7375-7378.
- 17 K. O. Marichev and J. M. Takacs, *ACS Catal.*, 2016, **6**, 2205-2210.
- 18 Y. Zhang, C.-S. Lim, D. S. B. Sim, H.-J. Pan and Y. Zhao, *Angew. Chem. Int. Ed.*, 2014, **53**, 1399-1403.
- 19 V. Froidevaux, C. Negrell, S. Caillol, J.-P. Pascault and B. Boutevin, *Chem. Rev.*, 2016, **116**, 14181-14224.
- 20 C. Gunanathan and D. Milstein, *Angew. Chem. Int. Ed.*, 2008, **47**, 8661-8664.
- 21 D. Ruiz, A. Aho, T. Salorant, K. Eränen, J. Wärnä, R. Leino, D. Yu. Murzin, *Chem. Eng. J.*, 2017, **207**, 739-749.
- 22 A. Fischer, M. Maciejewski, T. Bürgi, T. Mallat and A. Baiker, *J. Catal.*, 1999, **183**, 373-383.
- 23 Takanashi, T., Nakagawa, Y. & Tomishige, K. *Chem. Lett.*, 2014, **43**, 822-824.
- 24 T. Wang, J. Ibañez, K. Wang, L. Fang, M. Sabbe, C. Michel, S. Paul, M. Pera-Titus and P. Sautet, *Nat. Catal.*, 2019, **2**, 773-779.
- 25 L. C. Liu and A. Corma, *Chem. Rev.*, 2018, **118**, 4981-5079.

- 26 C. A. Schoenbaum, D. K. Schwartz and J. W. Medlin, *Acc. Chem. Res.*, 2014, **47**, 1438-1445.
- 27 P. X. Liu, R. X. Qin, G. Fu and N. F. Zheng, *J. Am. Chem. Soc.*, 2017, **139**, 2122-2131.
- 28 B. Gu, V. V. Ordonsky, M. Bahri, O. Ersen, P. A. Chernavskii, D. Filimonov and A. Y. Khodakov, *Appl. Catal. B*, 2018, **234**, 153-166.
- 29 B. Gu, M. Bahri, O. Ersen, A. Y. Khodakov and V. V. Ordonsky, *ACS Catal.*, 2019, **9**, 991-1000.
- 30 S. Imm, S. Bähn, L. Neubert, H. Neumann and M. Beller, *Angew. Chem. Int. Ed.*, 2010, **49**, 8126-8129.
- 31 G. Guillena, D.J. Ramón, M. Yus, *Angew. Chem. Int. Ed.* 2007, **46**, 2358-2364.
- 32 G. Jaiswal, V.G Landge, D. Jagadeesan, E. Balaraman, *Nat. Commun.* 2017, **8**, 2147.
- 33 D. Ruiz, A. Aho, T. Saloranta, K. Eränen, J. Wärnä, R. Leino and D. Y. Murzin, *Chem. Eng. J.*, 2017, **307**, 739-749.
- 34 J.P Bonnelle, J Grimblot., A. D'huysser, *J. Electron Spectr.*, 1975, **7**, 151-162.
- 35 D.G. Castner, P.R. Watson, and I.Y. Chan, *J. Phys. Chem.* 1989, **93**, 3188-3194.
- 36 O. O. James and S. Maity, *J. Pet. Technol. Altern. Fuels*, 2016, **7**, 1-12.
- 37 W. Chu, P.A. Chernavskii, L. Gengembre, G.A. Pankina, P. Fongarland, A.Y., Khodakov, *J. Catal.* 2007, **252**, 215-230
- 38 A. Baiker, *Stud. Surf. Sci. Catal.*, 1988, **41**, 283-290.
- 39 R. J. Shi, F. Wang, Tana, Y. Li, X. M. Huang and W. J. Shen, *Green Chem.*, 2010, **12**, 108-113.
- 40 T. O. Eschemann and K. P. Jong, *ACS Catal.*, 2015, **5**, 3181-3188.

41 M. D. Argyle and C. H. Bartholomew, *Catalysts*, 2015, **5**, 145-269.

42 C. Lancelot, V.V. Ordonsky, O. Stéphan, M. Sadeqzadeh, H. Karaca M. Lacroix, D. Curulla-Ferré, F. Luck, P. Fongarland, A. Griboval-Constant, A.Y. Khodakov, *ACS Catal.*, 2014, **4**, 4510-4515.

43 H. Karaca, O.V.Safonov, S. Chambrey, P. Fongarland, P. Roussel, A. Griboval-Constant, M. Lacroix, A.Y. Khodakov, *J. Catal.*, 2011, **277**, 14-26.

Table 1 Physical properties of supported fresh and Bi promoted cobalt catalysts

Catalyst	S_{BET}^a (m ² /g)	V_{tot}^b (cm ³ /g)	D_{meso}^c (nm)	Particle size (nm)			Total H ₂ consumption (mmol/g) ^g	Metallic surface area (m ² /g) ^h	Co _(CO) / Co (%) ^h
				$d_{\text{Co}_3\text{O}_4}^d$	d_{Co}^e	$d_{\text{Co}}^{\text{TEM}f}$			
Co/Al ₂ O ₃	120.72	0.39	10.55	13.2	9.9	10.0	0.87	7.73	1.14
Co0.5Bi/Al ₂ O ₃	121.32	0.40	10.61	13.9	10.4	10.2	1.43	5.6	0.83
Co1.0Bi/Al ₂ O ₃	122.23	0.42	10.82	12.8	9.6	10.8	1.5	4.5	0.67
Co2.0Bi/Al ₂ O ₃	119.04	0.39	10.85	13.0	9.8	10.3	1.3	3.1	0.46
Co5.0Bi/Al ₂ O ₃	120.66	0.38	10.28	14.1	10.6	10.5	1.52	1.2	0.18
Bi/Al ₂ O ₃	124.06	0.41	10.45	-	-	-	0.67	-	-

^a BET surface area measured by N₂ adsorption-desorption;

^b Pore volume of pores;

^c Pore diameter in mesoporous region;

^d The average particle size of Co₃O₄ is calculated by Scherrer equation using X-ray line broadening method;

^e Determined from the molar volume correction of size using $d(\text{Co}) = 0.75 d(\text{Co}_3\text{O}_4)$;

^f Determined from randomly selected particles in HAADF-STEM;

^g The total H₂ consumption from H₂-TPR analysis;

^h Obtained from CO chemisorption measurement.

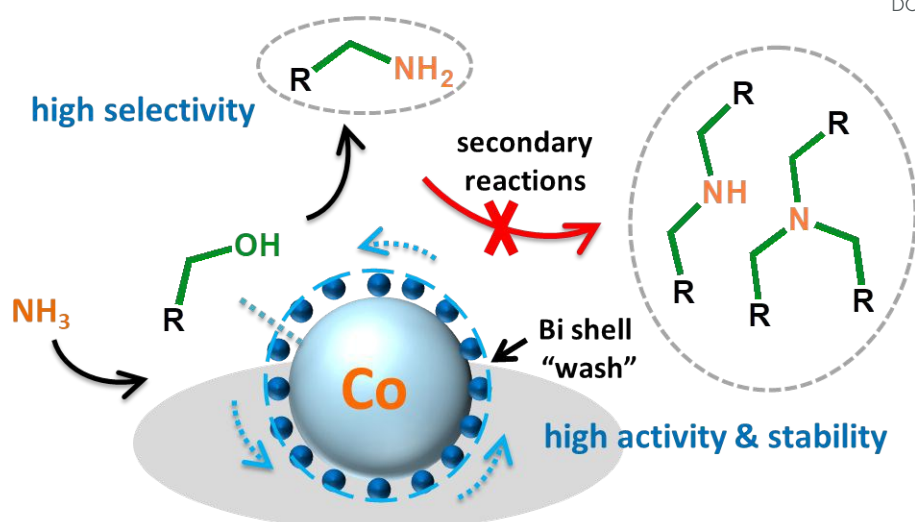


Figure 1 Effect of Bi promotion in amination of alcohols

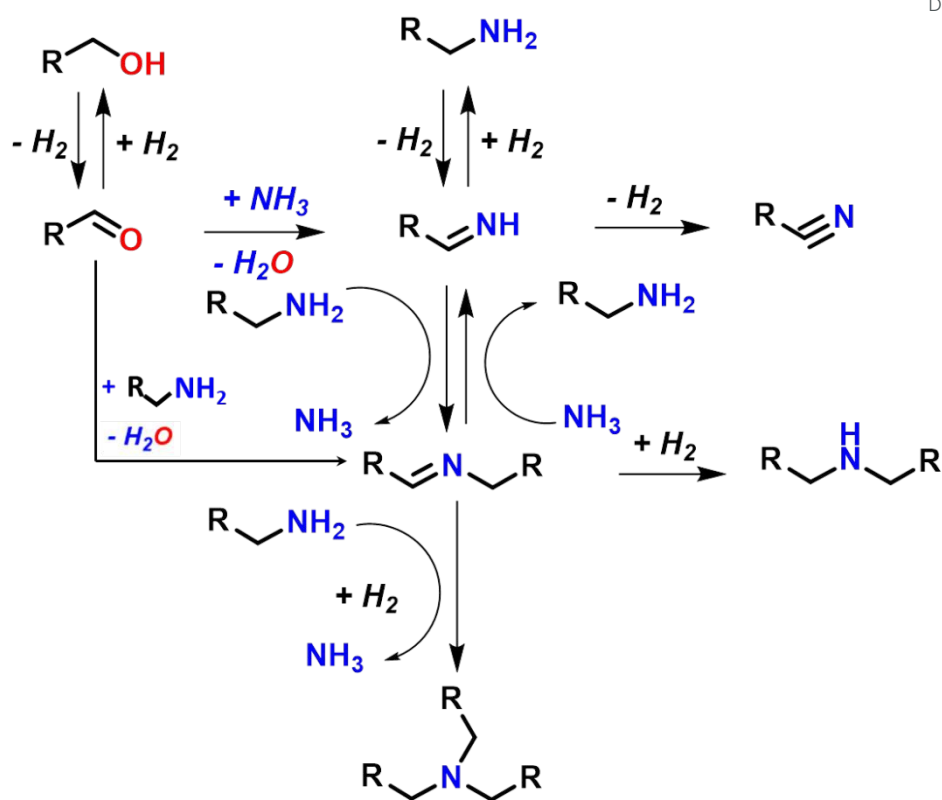


Figure 2 Reaction paths in amination of alcohols over supported metal catalyst

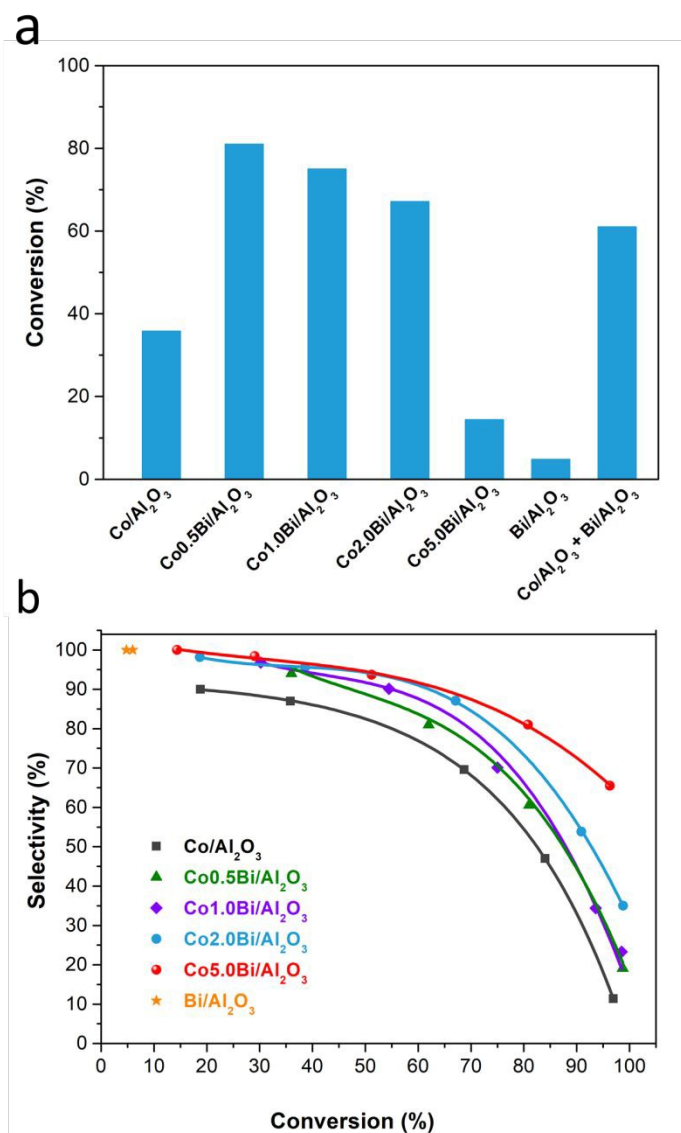


Figure 3 Catalytic conversion modification by Bi promotion (a) and selectivity-conversion curves (b) for liquid phase amination of 1-octanol over activated Co/Al₂O₃ and bimetallic Co_xBi/Al₂O₃ catalysts (1-octanol, 0.84 g; molar ratio of 1-octanol/NH₃/H₂ = 1/4.5/0.85; P_{H₂} = 3 bar; catalyst amount, 100 mg; reaction temperature, 180 °C; time, 0-48 h; no solvent used).

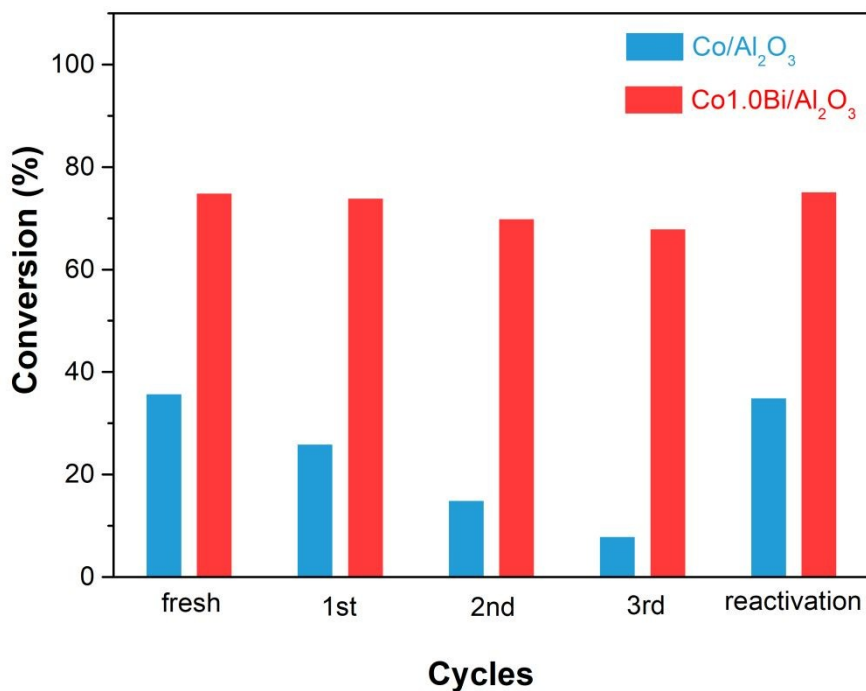


Figure 4 Catalytic reusability and stability for liquid phase amination of 1-octanol over activated Co/Al₂O₃ and Co1.0Bi/Al₂O₃ catalysts (1-octanol, 0.84 g; molar ratio of 1-octanol/NH₃/H₂ = 1/4.5/0.85; P_{H₂} = 3 bar; catalyst amount, 100 mg; reaction temperature, 180 °C; time, 5 h; no solvent used; reactivation condition: 400 °C calcination under air followed by H₂ activation at 450 °C).

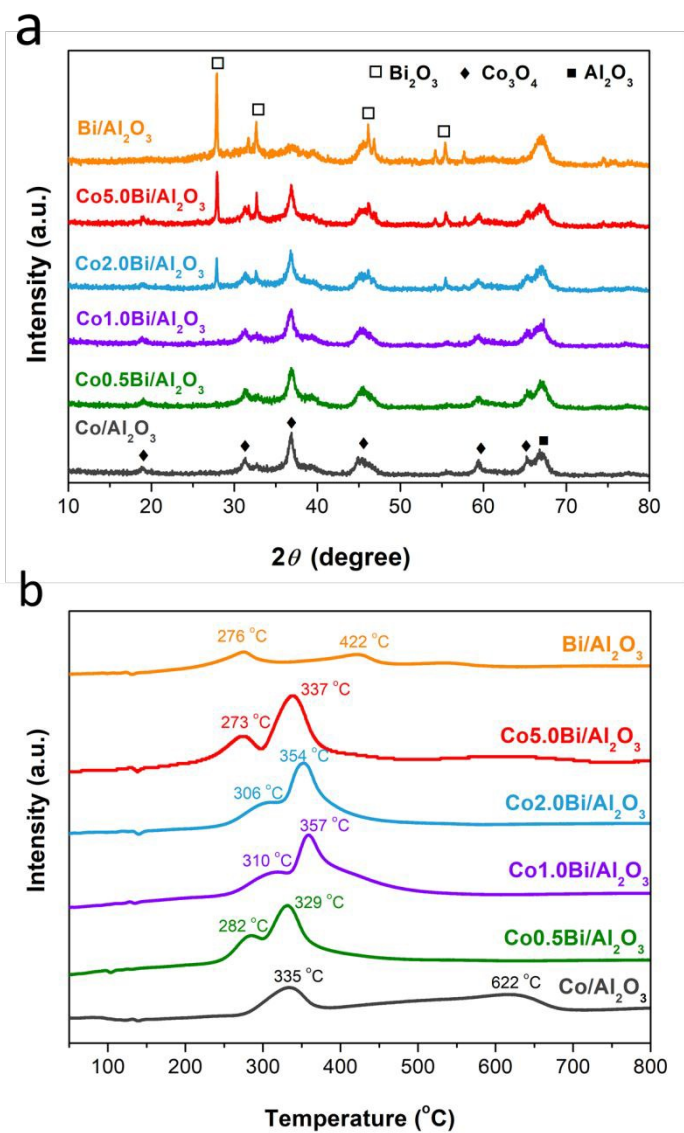


Figure 5 XRD patterns (a) and H₂-TPR profiles (b) of oxidized Co/Al₂O₃, Bi/Al₂O₃ and bimetallic Co_xBi/Al₂O₃ catalysts.

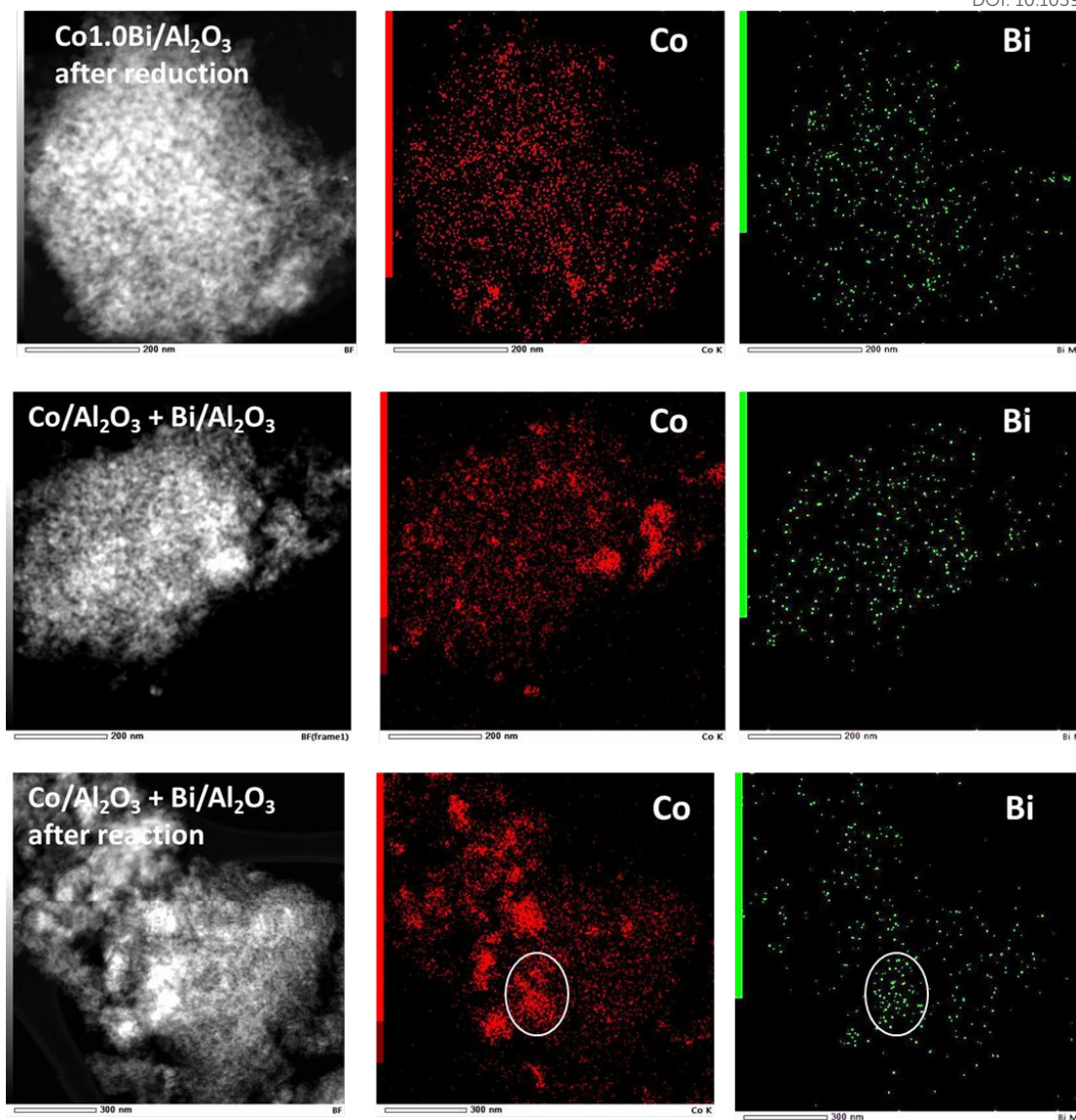


Figure 6 HAADF-STEM images and EDX mapping of Co and Bi of reduced $\text{Co}_{1.0}\text{Bi}/\text{Al}_2\text{O}_3$ catalyst and mechanical mixture $\text{Co}/\text{Al}_2\text{O}_3 + \text{Bi}/\text{Al}_2\text{O}_3$ before and after reaction of amination

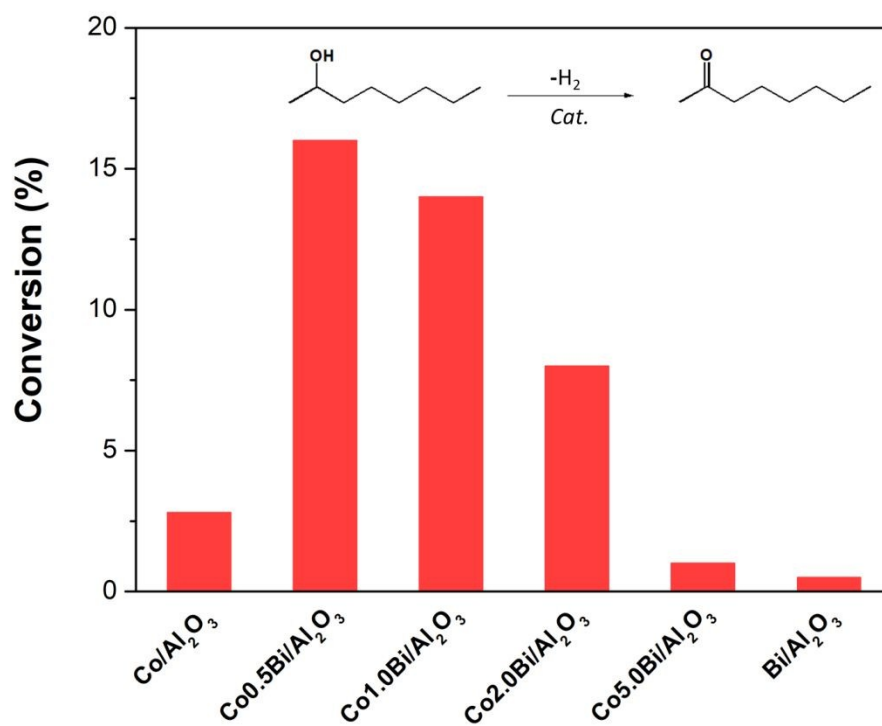


Figure 7 Comparison of catalytic conversion for liquid phase dehydrogenation of 2-octanol over activated Co/Al₂O₃, Bi/Al₂O₃ and bimetallic Co_xBi/Al₂O₃ catalysts (2-octanol, 50 mg; toluene, 1 g; catalyst amount, 50 mg; reaction temperature, 140 °C; time, 15 h).

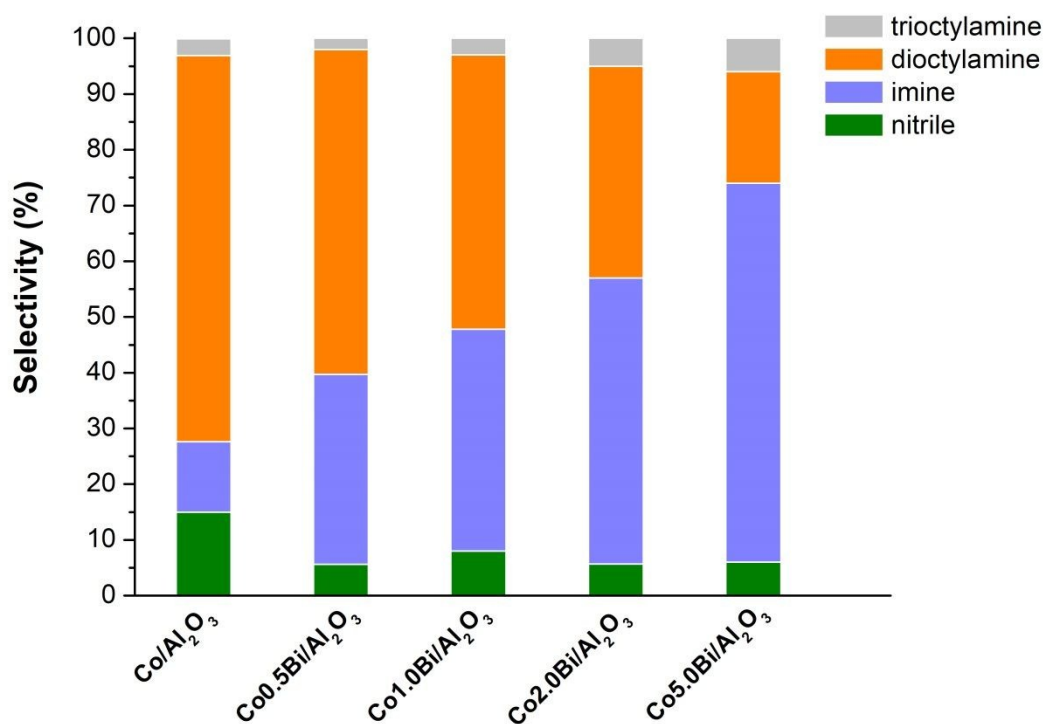


Figure 8 Model reaction of 1-octylamine transformation over activated Co/Al₂O₃ and bimetallic Co_xBi/Al₂O₃ catalysts at a conversion of < 10% (1-octylamine, 1 mL; catalyst amount, 20 mg; molar ratio of 1-octanol/NH₃/H₂ = 1/4.5/0.85; P_{H₂} = 3 bar; reaction temperature, 180 °C; time, 0-4 h; no solvent used).